Atmospheric Pollution Research 17 (2026) 103202

Contents lists available at ScienceDirect

Atmospheric Pollution Research

journal homepage: www.elsevier.com/locate/apr

Soil drivers of NH_3 emissions in a fertilized sunflower agroecosystem

Eszter Tóth [a], János Balogh [b], Zoltán Bozóki [c,d], László Horváth [d,*], Zoltán Nagy [b,e], Zsófia Oltvári [c], Tünde Takács [f,g], Krisztina Pintér [b,e]

[a] Institute for Soil Sciences and Agricultural Chemistry, Centre for Agricultural Research, Fehérvári út 132-144, Budapest, H-1116, Hungary
[b] Department of Plant Physiology and Plant Ecology, Institute of Agronomy, Hungarian University of Agriculture and Life Sciences, Páter Károly utca 1, Gödöllő, H-2100, Hungary
[c] Department of Optics and Quantum Electronics, University of Szeged, Dóm tér 9, Szeged, H-6720, Hungary
[d] HUN-REN-SZTE Research Group for Photoacoustic Monitoring of Environmental Processes, University of Szeged, Dóm tér 9, Szeged, H-6720, Hungary
[e] HUN-REN-MATE Agroecology Research Group, Hungarian University of Agriculture and Life Sciences, Páter Károly utca 1, Gödöllő, H-2100, Hungary
[f] Department of Soil Biology, Institute for Soil Sciences and Agricultural Chemistry, Centre for Agricultural Research, Fehérvári út 132-144, Budapest, H-1116, Hungary
[g] Department of Soil, Water and Natural Sciences, Albert Casimir Faculty at Mosonmagyaróvár, Széchenyi István University, Lucsony utca 15-17, Mosonmagyaróvár, H-9200, Hungary

ARTICLE INFO

Keywords:
Ammonia volatilization
Soil NH_3 flux
Random forest
SHAP analysis
Soil depth effects

ABSTRACT

Ammonia (NH_3) volatilization represents a major pathway of reactive nitrogen loss in agroecosystems, yet the soil controls governing its variability remain insufficiently understood. In this study, we quantified soil-atmosphere NH_3 fluxes in a fertilized sunflower field in Hungary using multi-point field measurements (20 locations, 18 campaigns), combined with detailed soil, canopy, and microclimatic observations. To identify the dominant drivers of NH_3 flux variability, we applied a Random Forest modeling approach complemented by SHAP-based interpretation. The RF and SHAP analyses indicated non-linear, modelled associations of NH_3 flux with soil temperature, moisture, humus content, and the $[NH_4^+]/[H^+]$ proxy (Γ). Notably, properties measured in deeper soil layers (20–30 cm) contributed to the model predictions, indicating associations between NH_3 flux variability and vertically structured soil processes rather than surface conditions alone. NO_3^- emerged as a conditional, state-dependent model-associated indicator, potentially reflecting broader N-transformation dynamics and covariance with soil moisture and temperature rather than a direct causal effect on NH_3 volatilization. These findings emphasize that NH_3 fluxes arise from complex interactions among soil chemical status, microclimate, and nitrogen transformation processes within the soil profile. The results demonstrate that data-driven approaches can provide new insights into nitrogen cycling processes in agroecosystems.

1. Introduction

The enrichment of ecosystems with reactive nitrogen (N_r) has emerged as a major environmental challenge of the Anthropocene. Reactive nitrogen compounds exert multiple adverse effects: they reduce air quality through the formation of fine particulate matter, threaten biodiversity via aquatic eutrophication and soil contamination, acidify soils, and contribute to nitrate (NO_3^-) contamination of groundwater. In the atmosphere, nitrous oxide (N_2O) is both a potent greenhouse gas and a driver of stratospheric ozone depletion, whereas ammonia (NH_3) volatilization plays a central role in atmospheric aerosol formation and nitrogen deposition (Galloway et al., 2003; Sutton et al., 2013).

The global expansion of synthetic fertilizer use since the advent of the Haber-Bosch process has intensified the nitrogen cascade. The global production of NH_3 was estimated at ~150 million metric tons (Statista, 2025), and a significant fraction of this reactive nitrogen is released back to the environment rather than assimilated by crops. Estimates suggest that the overall nitrogen use efficiency (NUE) of synthetic fertilizers is below 50% at the global scale, with volatilization and leaching representing major loss pathways (Bindraban et al., 2020; Coskun et al., 2017).

Among these losses, NH_3 emissions are of particular concern. Fertilizer-derived NH_3 volatilization contributes substantially to the total nitrogen budget of croplands, often exceeding losses in the form of

* Corresponding author.
E-mail addresses: toth.eszter@atk.hun-ren.hu (E. Tóth), Balogh.Janos@uni-mate.hu (J. Balogh), zbozoki@physx.u-szeged.hu (Z. Bozóki), horvathl@titan.physx.u-szeged.hu (L. Horváth), Nagy.Zoltan@uni-mate.hu (Z. Nagy), ozsegyetem@gmail.com (Z. Oltvári), takacs.tunde@atk.hun-ren.hu (T. Takács), Pinter.Krisztina@uni-mate.hu (K. Pintér).

https://doi.org/10.1016/j.apr.2026.103202
Received 30 April 2026; Received in revised form 16 September 2026; Accepted 16 September 2026
Available online 17 September 2026

N_2O; emission rates peak shortly after fertilizer application and are strongly modulated by fertilizer formulation, soil chemical properties (especially pH and cation exchange capacity), microclimatic factors (temperature, soil moisture, wind), and crop canopy development (Génermont and Cellier, 1997; Nelson et al., 2017; Sommer et al., 2004; Zhan et al., 2020). Volatilization tends to be highest from urea-based products but varies among NH_4^+ salts and mixed fertilizers (He et al., 1999; Ma et al., 2021). The relationship between N dose and NH_3 emission is non-linear, with disproportionately high losses at elevated inputs (Jiang et al., 2017).

Beyond fertilizer type and placement, soil chemistry exerts first-order control on NH_3 losses. Soil pH governs the NH_4^+/NH_3 equilibrium; higher surface pH intensifies volatilization, whereas management that buffers acidity or modifies microsite pH can reduce emissions. On acidic soils, organic fertilizer applications have been shown to lower NH_3 loss, likely via enhanced buffering and altered microsite conditions (Gan et al., 2025). The size and vertical distribution of inorganic N pools also shape emission timing and magnitude: surface enrichment of NH_4^+ correlates with higher volatilization, while deeper placement reduces exposure to alkaline microsites and atmospheric exchange (Zhong et al., 2021). Changes in labile soil C-N fractions interact with these pools and microbial pathways, influencing both NH_3 volatilization and N_2O emission (Zhang et al., 2022).

Soil microclimate is another key regulator. Moisture and temperature modulate hydrolysis, diffusion processes and boundary-layer humidity; manipulations such as plastic film mulching, residue retention and irrigation timing shift surface water and thermal regimes and thereby NH_3 fluxes (Chae et al., 2022; Li et al., 2021). Warming experiments in paddy soils show that elevated temperature accelerates N transformations and amplifies both NH_3 volatilization and N_2O emissions, consistent with temperature-sensitive NH_4/NH_3 partitioning (Deng et al., 2023).

Management can leverage these controls. Cover cropping, depending on the species composition, with reduced N rates mitigates NH_3 loss and greenhouse gas emissions by regulating labile C and N fractions without compromising yields, while side-deep or root-zone targeted placement moves urea/NH_4^+ away from high-pH surface microsites and improves NUE; rate, placement and timing jointly determine volatilization dynamics, with split and non-surface applications limiting early peaks (Sun et al., 2022; Wang et al., 2021; Zhong et al., 2021). Plant canopy development interacts with soil processes: leaf area index (LAI) and crop height affect near-surface turbulence and microclimate, which in turn modulate NH_3 exchange (Sun et al., 2022).

Alongside NH_3, croplands are important sources of CO_2 and N_2O. CO_2 fluxes are tightly coupled to soil respiration, organic matter turnover and plant activity, whereas N_2O arises chiefly from microbial nitrification-denitrification; both respond to the same temperature-moisture drivers that regulate NH_3 (Butterbach-Bahl et al., 2013). Overall, evidence converges on a process-level picture in which NH_3 peaks shortly after N application and is modulated by (i) soil pH and buffering capacity, (ii) the size and lability of NH_4^+ and organic C pools, (iii) surface temperature-moisture states and (iv) fertilizer-soil-root contact geometry. Management addressing these levers, cover crops, side-deep placement, mulching, irrigation adjustments and organic amendments, can simultaneously raise NUE and suppress NH_3 while co-benefiting (or at least not worsening) N_2O and CO_2 outcomes (Chae et al., 2022; Gan et al., 2025; Li et al., 2021; Sun et al., 2022; Zhong et al., 2021). Despite extensive research, the role of subsoil layers in NH_3 volatilization remains poorly understood.

Soil NH_3 fluxes arise from strongly nonlinear, multi-factor interactions among soil physical (e.g., VWC, soil temperature), and chemical drivers (e.g. pH, NH_4^+, mineral N pools, together with substrate availability, soil organic matter, and canopy state (LAI, height of biomass). Such interactions often produce thresholds and non-additive effects that are captured more effectively by data-driven models, especially Random Forest (RF) and related gradient-boosting approaches, than by linear or fixed-form empirical schemes. Across diverse systems, recent studies show that RF improves predictions of daily and cumulative fluxes and yields robust variable-importance rankings, particularly when soil physical (VWC), soil chemical (pH, NH_4^+, NO_3^-), and management predictors (application method/timing, inhibitors, water supply) are combined (Adjuik and Davis, 2022; Dhaliwal et al., 2025; Favrot et al., 2025; Hurtado et al., 2024; Philibert et al., 2013; Saha et al., 2021; Uyekawa et al., 2025).

The aim of this study was to identify the key soil and plant factors controlling NH_3 emissions from a fertilized sunflower field. We focused on disentangling the relative influence of soil physical and chemical properties, including VWC, soil temperature, NH_4^+, NO_3^-, total nitrogen, humus, and pH, together with vegetation characteristics such as leaf area index (LAI) and plant height. These variables were analyzed as measured at three soil depth intervals (0–10, 10–20, and 20–30 cm), in order to determine which soil layer exerts the strongest influence on net NH_3 fluxes and how vertical soil heterogeneity shapes gaseous nitrogen losses. The primary objective of this study was not to derive a complete emission budget, but to identify the key environmental controls governing NH_3 flux variability.

2. Materials and methods

2.1. The site of investigations

Measurements and sampling were conducted in an arable field near Kartal, at the Gödöllő Experimental Farm PLC, during the 2024 growing season (March to October). The site coordinates were $\varphi = 47^\circ\ 39'\ 42.56''$, $\lambda = 19^\circ\ 31'\ 43.21''$, at an elevation of 153 m. The climate is continental, with an average annual precipitation (1991-2020) between 550 and 600 mm $year^{-1}$. During the study period, the amount of precipitation was 350 mm.

The soil was classified as a Haplic Phaeozem (Humic, Pantoloamic) according to the International Union of Soil Sciences World Reference Base for Soil Resources classification system (IUSS Working Group WRB, 2022). The soil texture was as follows: clay 32.3%, silt 49.1%, and sand 18.6%, which corresponds to a silty clay loam according to the USDA textural classification.

For soil flux sampling, collars were installed on the soil surface. These remained in place throughout the season, except during certain cultivation operations, to minimize errors in flux estimation caused by soil disturbance. The arrangement of the collars is shown in Fig. 1.

On 20 March 2024, 54 kg N ha^{-1} in the form of granulated calcium ammonium nitrate (CAN) was applied to the soil surface. Sunflower

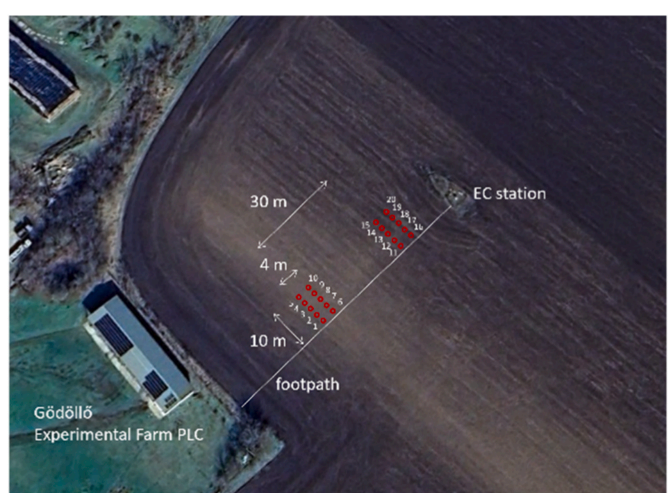

Fig. 1. Measurement site and collar arrangement near the CO_2 Eddy Covariance station.

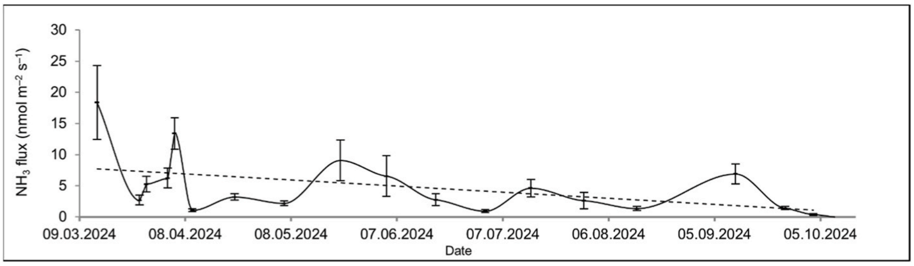

Fig. 2. Temporal variation in mean soil NH_3 flux across the 20 sampling points. Error bars represent the standard error (1σ). The solid line shows the PCHIP interpolation, and the dotted line represents the linear regression, $y = -0.0327x + 10.16$, where x is the day of year (DOY) and y is NH_3 flux ($R^2 = 0.218$, $p = 0.05$).

(*Helianthus annuus* L., cv. SY Bacardi) was sown at a density of 60,000 plants ha^{-1} on 14 April. After the sunflower harvest on 3 September, an additional 15 kg N ha^{-1} was applied on 19 September as part of a mixed N-P-K fertilizer containing diammonium hydrogen phosphate [$(NH_4)_2HPO_4$] as the N-P component and an additional potassium-containing component (KCl).

2.2. Soil physical properties

Soil moisture was measured with an ML3 ThetaProbe Soil Moisture Sensor (Delta-T Devices, UK) using electrical conductivity to estimate volumetric water content. Soil temperature was recorded with a Brannan thermometer (accuracy ±0.1 °C). To estimate the daily course of soil temperature, measurements were taken at the eddy covariance CO_2 flux measurement site located near the experimental sampling points using a Campbell CS650 sensor connected to a CR3000 data logger.

2.3. Plant characteristics

Plant height was measured at 20 locations using a measuring tape, while the leaf area index values at 7 permanent locations were estimated by using an AccuPAR LP-80 Ceptometer (METER Group Pullman, WA). Measurements were conducted approximately every 7-10 days (DOY 140-276), with shorter intervals following fertilization and major precipitation events.

2.4. Soil chemistry analysis

After each soil flux measurement, three soil samples were collected from each of the 20 sampling points at three depths (0–10, 10–20, and 20–30 cm). On the first sampling day (14 March 2024), all samples were analyzed individually. On subsequent days, composite samples were prepared separately from sampling points 1-10 and 11-20.

After drying, the soil samples were ground with a 2 mm jaw crusher for chemical analyses. Air drying before extraction may alter mineral N concentrations, particularly through partial NH_3 loss from ammonium-rich soils (Rochester et al., 1991). Therefore, the reported NH_4^+ concentrations represent operationally defined values measured in dried soil rather than direct estimates of in situ soil-solution NH_4^+ concentrations. Humus content was determined using the modified Walkley-Black method for organic carbon (FAO, 2020). Total nitrogen (tot N) was quantified using a modified Kjeldahl method (ISO, 1995). NH_4^+ and NO_3^- concentrations were analyzed using wet chemical methods (Bremner and Keeney, 1966). Soil pH was measured with a MultiLine meter after sample preparation according to the Hungarian Standard (MSZ, 1978).

During the measurement period, soil solution pH(H_2O) values measured across the 20 sampling locations (n = 18 campaigns) ranged between 7.15 and 8.13, with a mean value of 7.80. This corresponds to approximately one order of magnitude variation in hydrogen ion concentration, which is expected to significantly influence the NH_4^+/NH_3 equilibrium and thus the potential for ammonia volatilization.

2.5. Soil gas net flux measurements

NH_3 fluxes were measured using a Picarro G2103 analyzer (Picarro Inc., Santa Clara, CA, USA) based on Cavity Ring-Down Spectroscopy. Measurements were conducted using an open dynamic chamber (diameter = 10.5 cm, height = 20 cm, A ≈ 86.6 cm^2) with a flow rate exceeding 1.5 standard liters per minute at 1.013 bar pressure.

Soil moisture was measured using an ML3 ThetaProbe Soil Moisture Sensor (Delta-T Devices, UK), which estimates volumetric water content (VWC) based on electrical conductivity. Soil temperature (t) was recorded using a Brannan thermometer (accuracy ±0.1 °C).

The chamber was placed on pre-installed collars on bare, vegetation-free soil surfaces to ensure that the measured fluxes represented soil emissions only. The smaller-diameter chamber used for NH_3 measurements was placed inside the collar, ensuring that gas measurements were taken at the same points. Soil fluxes were measured on all 20 sampling points, with 18 sampling occasions. Measurements were carried out between 09:00 and 10:30 UTC to minimize potential bias from diurnal soil temperature fluctuations. As shown in Table 1, the mean temperatures recorded at different depths during this period closely matched the corresponding daily averages, indicating that errors associated with short-term soil temperature variability were effectively avoided.

While continuous measurements would be required to fully resolve temporal emission dynamics, temporally discrete field measurements are widely applied and are suitable for identifying dominant environmental controls and interaction effects, which is the primary focus of the present study.

To determine soil emission trends, we applied the shape-preserving Piecewise Cubic Hermite Interpolating Polynomial (PCHIP) method (Fritsch and Carlson, 1980; Fritsch and Butland, 1984), as implemented in SciPy (Virtanen et al., 2020), in addition to linear combinations. Unlike conventional cubic spline interpolation, which can produce spurious oscillations and even negative values between data points, PCHIP preserves the monotonicity and non-negativity of the observed data, thereby providing a more realistic representation of flux dynamics.

The analysis was based on approximately 3000 flux, soil physical, and soil chemical measurements. The aim was to determine the dependence of soil NH_3 fluxes on various physical, chemical, and plant

Table 1
Comparison of daily average soil temperature with values measured at different UTC times.

Soil temperature (°C)				
Depth	−7 cm	−20 cm	−30 cm	Mean of 3 depths
Daily Mean	20.1	19.6	19.3	19.7
9:00	19.3	18.6	18.9	18.9
9:30	19.9	18.6	18.9	19.1
10:00	20.5	18.7	18.8	19.3
10:30	21.1	18.8	18.8	19.6

parameters. These are presented in Table 2.

In addition to the measured values, we introduced a derived variable, the so-called soil gamma, because the soil compensation point concentration (Farquhar et al., 1980), which controls soil NH_3 exchange, is determined using a formula that combines Henry's law and dissociation equilibria (Personne et al., 2009; Sutton et al., 1994):

$$[NH_3] = K_H \times K_A \times \left\{ \exp\left[\frac{\Delta G_H^0 + \Delta G_A^0}{R} \left(\frac{1}{298.15} - \frac{1}{T} \right) \right] \right\} \times \Gamma,$$

where K_H and K_A are the Henry's constant for NH_3 between the soil aqueous phase and the atmosphere, and the dissociation constant, respectively; ΔG_H^0 and ΔG_A^0 are the corresponding standard Gibbs free energies. The gamma factor ($\Gamma = [NH_4^+]/[H^+]$), which directly determines the soil-air compensation point concentration, would likely emerge as a top predictor, integrating the effects of both NH_4^+ and acidity on NH_3 emissions.

The $[NH_4^+]/[H^+]$ ratio (Γ) in the soil solution could not be directly determined. Instead, we calculated an apparent ammonium-to-hydrogen concentration ratio based on the NH_4^+ concentration measured in soil extracts (expressed as mg NH_4^+ kg^{-1} dry soil) and the hydrogen ion concentration (μmol L^{-1}) derived from the extract pH.

Γ is not dimensionally rigorous and should be interpreted as a relative index rather than an absolute physicochemical parameter. While this parameter does not represent the true Γ of the soil solution, it is assumed to be proportional to it and is therefore used here as an operational proxy.

Flux measurements were conducted at discrete time points rather than continuously; therefore, cumulative emission estimates should be interpreted as approximate. As a consequence, cumulative flux estimates should be interpreted as approximate rather than exhaustive representations of total emissions.

Measurements were consistently performed within a narrow time window (09:00-10:30 UTC), corresponding closely to the daily mean soil temperature, thereby reducing systematic bias associated with diurnal variability.

Although no unfertilized control plot was included, this does not limit the interpretation of NH_3 fluxes. Ammonia exchange is bidirectional and controlled by the compensation point, which depends on the nitrogen status of the system (Massad et al., 2010; Sutton et al., 2013). Under low nitrogen input conditions, this typically results in low emission potentials and often net deposition, as also demonstrated by field measurements over non-fertilized grasslands in Central Europe (Horváth et al., 2005). Therefore, the observed fluxes can be primarily attributed to fertilization and associated environmental drivers.

2.6. Machine learning statistical modeling

Soil NH_3 fluxes were analyzed using a suite of machine-learning and statistical models (Stryker et al., 2025). The primary predictor set comprised volumetric water content (VWC), soil temperature, NO_3^- concentration, total nitrogen, humus content, leaf area index (LAI), canopy height, and the Γ index associated with the NH_3 compensation point. Soil chemical properties were measured at depths of 0–10, 10–20, and 20–30 cm. For the primary analysis of relationships between NH_3 flux and environmental variables, values from the three soil depths were averaged. The resulting dataset contained 360 observations derived from 20 sampling points and 18 measurement campaigns.

Five supervised regression algorithms were compared: Random Forest (RF), Ordinary Least Squares (OLS), Partial Least Squares Regression (PLSR), Ridge regression, and Lasso regression. Predictors were standardized by Z-score transformation (Andrade, 2021) within each training fold for OLS, Ridge regression ($\alpha = 1$), Lasso regression (Least Absolute Shrinkage and Selection Operator; $\alpha = 0.1$, max_iter = 10,000), and PLSR, whereas the RF models were fitted to the unscaled predictors. The models were implemented using scikit-learn; see Scikit-learn Developers (2025a) for PLSR, Scikit-learn Developers (2025d) for OLS, Ridge, and Lasso, and Scikit-learn Developers (2025f) for RF. The number of retained PLSR components (1–10) was selected by five-fold inner cross-validation. All RF models comprised 500 trees, with $\sqrt{p}$ candidate predictors considered at each split (Scikit-learn Developers, 2025f).

Model performance was evaluated using shuffled 10-fold cross-validation with a fixed random state (shuffle = True, random_state = 42; Scikit-learn Developers, 2025b). The coefficient of determination (R^2), root mean squared error (RMSE), and mean absolute error (MAE) were calculated from held-out predictions and are reported as mean ± SD across folds (Scikit-learn Developers, 2025e). In addition, a single reproducible 80/20 train–test split (random_state = 42) was used to fit a consistent RF model for SHAP-based interpretation rather than as the primary estimate of predictive performance.

Because measurements were repeated at the same sampling points, random cross-validation may have allowed some information overlap between the training and validation folds. Consequently, the resulting performance estimates may be slightly optimistic and should be interpreted as indicative rather than as estimates based on fully independent observations. A grouped cross-validation strategy based on sampling location could provide a more stringent assessment of spatial generalization.

To assess depth-resolved soil controls on NH_3 flux, a separate analysis was performed using Γ, NO_3^- concentration, total nitrogen, and humus content measured individually at 0–10, 10–20, and 20–30 cm. These were the soil chemical predictors available separately for all three depths across the 20 sampling points and 18 measurement campaigns, resulting in 360 observations. This analysis used the same modeling and cross-validation procedures described above. RF was evaluated alongside OLS, Ridge, and Lasso, and PLSR as benchmark models.

Predictor importance was quantified using three complementary approaches: (1) impurity-based RF feature importance, calculated as the accumulated mean decrease in impurity and summarized as the mean ± SD across the 10 cross-validation models (Scikit-learn Developers, 2025c); (2) SHAP (SHapley Additive Explanations) values calculated using TreeExplainer (Lundberg, 2018); and (3) permutation importance, calculated for individual predictors and after aggregation by soil depth. For the single-split RF model, global SHAP importance was calculated as the mean absolute SHAP value across observations, representing the average magnitude of each predictor's contribution to model predictions.

One-dimensional Partial Dependence Plots (PDPs) were generated from the depth-resolved RF model to examine the modelled associations of NO_3^- at 0–10, 10–20, and 20–30 cm soil depths. The two-dimensional PDPs were generated separately from the primary RF model, which included VWC, soil temperature, and NO_3^- averaged across the three sampled soil depths. These plots therefore show the joint modelled associations of depth-averaged NO_3^- with VWC and soil temperature.

Table 2
Predictors used in the analysis.

Sign	Name	Unit
t	Soil temperature	°C
hc	Canopy height	m
VWC	Soil volumetric water content	%
WFPS	Water filled pore space	%
LAI	Leaf area index (one side)	m^2 m^{-2}
NH_4^+	Ammonium concentration at 0–10, 10–20, and 20–30 cm depths	mg kg^{-1}
NO_3^-	Nitrate concentration at 0–10, 10–20, and 20–30 cm depths	mg kg^{-1}
Tot N	Total nitrogen content at 0–10, 10–20, and 20–30 cm depths	mass %
Humus	Humus content at 0–10, 10–20, and 20–30 cm depths	mass %
pH	pH at 0–10, 10–20, and 20–30 cm depths	-
Γ	Proxy of $[NH_4^+]/[H^+]$ ratio at 0–10, 10–20, and 20–30 cm depths	M M^{-1}

The three importance measures were treated as complementary because they quantify different aspects of predictor relevance. Permutation importance measures the decrease in model performance following predictor shuffling but can distribute importance among correlated predictors. SHAP provides global and observation-specific feature attributions and can represent nonlinear and interaction effects, although SHAP values must also be interpreted cautiously when predictors are correlated. SHAP was therefore used as the primary interpretability approach, while impurity-based and permutation importance were used as complementary robustness checks (Fisher et al., 2019; Lundberg and Lee, 2017; Molnar, 2020).

3. Results and discussion

The primary objective of this study was not to derive a fully resolved NH_3 emission budget, but to identify the key environmental drivers and soil controls governing NH_3 flux variability. While continuous measurements would be required to capture short-term peaks and diurnal variability in detail, temporally discrete flux measurements are widely used in field studies and are suitable for identifying relative patterns and driver-response relationships.

The temporal development of canopy height and LAI is shown in Supplementary Fig. S1, while the depth-resolved variation in NH_4^+, NO_3^-, pH, humus content, and total N is presented in Supplementary Figs. S2 and S3. The temporal variation in VWC and soil temperature is shown in Fig. 3.

3.1. All-season soil flux estimation from point measurements

Soil NH_3 fluxes over the 210-day period (14 March - 3 October 2024) were interpolated from 18 measurement days across 20 sampling points using the PCHIP method (Fig. 2). This method preserves monotonicity between observations and avoids the overshoot typical of standard cubic splines. The mean flux was 4.94 ± 0.25 nmol m^{-2} s^{-1}. Cumulative emission over the period amounted to 7.41×10^7 nmol m^{-2}, equivalent to 12.6 kg ha^{-1} (10.4 kg N ha^{-1}), with linear regression estimating a slightly higher value of 13.2 kg ha^{-1} (10.9 kg N ha^{-1}). This soil NH_3 emission is not negligible compared to the applied fertilizer amount (54 kg N ha^{-1} of CAN on 20 March 2024).

The estimated cumulative NH_3 emission corresponds to approximately 20% of the applied fertilizer N; however, this value should be interpreted with caution. Discrete sampling may overrepresent peak events relative to background fluxes. Due to the temporally discrete nature of the measurements, cumulative estimates should be regarded as indicative and primarily serve as context for interpreting environmental controls.

Previous studies consistently report low NH_3 volatilization losses from ammonium nitrate-based fertilizers such as calcium ammonium nitrate (CAN), typically only a few percent of applied nitrogen (Bouwman et al., 2002; Forrestal et al., 2016). Experimental evidence further confirms that nitrate-based fertilizers generally result in substantially lower NH_3 emissions than urea-based fertilizers (Forrestal et al., 2016; He et al., 1999) because nitrate does not directly contribute to the NH_4^+ pool or cause the localized increase in soil pH associated with urea hydrolysis. In contrast, urea hydrolysis generates NH_4^+ and temporarily increases microsite pH, thereby shifting the NH_4^+/NH_3 equilibrium towards volatile NH_3. At the same time, NH_3 losses increase with fertilizer application rate and may even exhibit non-linear (e.g., quadratic) responses under certain conditions, such as in paddy systems (Canatoy et al., 2024).

The cumulative seasonal NH_3 loss of approximately 10 kg N ha^{-1} following calcium ammonium nitrate application should be interpreted in the context of soil pH constraints on ammonia volatilization. While CAN fertilizer is generally regarded as a lower-emission alternative, this characterization primarily applies to acidic and near-neutral soils. Under neutral to alkaline conditions, volatilization losses from ammonium- and nitrate-based fertilizers can remain substantial and highly variable, depending on environmental drivers and management (Sommer et al., 2004; Pan et al., 2016). This response is mechanistically explained by the strong pH dependence of the NH_4^+/NH_3 equilibrium, which shifts exponentially toward NH_3 with increasing pH (Sommer and Hutchings, 2001).

Furthermore, field-scale evidence demonstrates that even fertilizers with lower intrinsic volatilization potential, such as CAN, can still exhibit measurable and occasionally substantial NH_3 losses when applied to soils with elevated pH, particularly under surface application and drying conditions (Bussink, 1994; Rochette et al., 2013). In addition, transient microsite effects following fertilizer dissolution, characterized by locally elevated ammonium concentrations and transient changes in microsite chemistry, can further amplify emission peaks that contribute disproportionately to cumulative seasonal losses (Rochette et al., 2013; Sommer et al., 2004). Given the soil pH range observed in this study (7.15-8.13) and the buffered, fine-textured characteristics of the investigated Haplic Phaeozem, the measured NH_3 loss (~10 kg N ha^{-1}, corresponding to ~20% of applied N) represents the upper end of reported emission ranges but remains fully consistent with established process understanding and published data for mineral fertilizers under alkaline conditions. Therefore, the observed magnitude should not be interpreted as anomalous, but rather as a plausible outcome under the given soil chemical and environmental conditions.

3.2. Qualitative assessment of flux – environment relationships

The temporal dynamics of soil-atmosphere fluxes of NH_3 exhibited clear links to meteorological and soil drivers. These meteorological and soil variables served as key environmental drivers of trace gas fluxes, influencing the dynamics of NH_3 volatilization, (e.g., Butterbach-Bahl et al., 2013; Misselbrook et al., 2005; Sanz-Cobena et al., 2014; Skiba et al., 2012). NH_3 flux showed a marked increase following the fertilization event on 20 March. Peaks in NH_3 volatilization coincided with periods of moderately elevated soil temperature and higher VWC, suggesting that warm and moist soil conditions facilitated the transfer of ammoniacal nitrogen from the soil solution to the atmosphere. Soil moisture strongly controls NH_3 emission. At low water content, limited

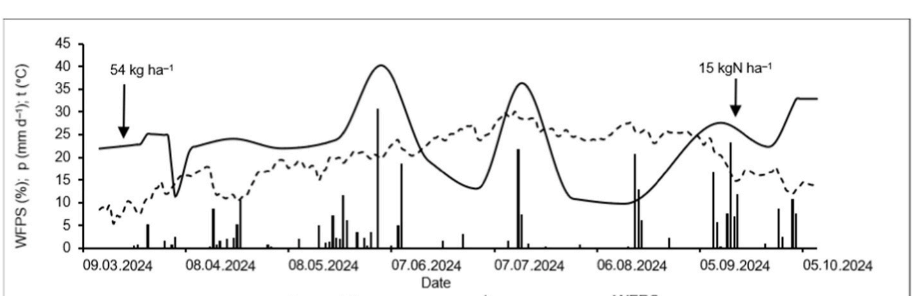

Fig. 3. Temporal variation of precipitation (p), water filled pore space (WFPS), and soil temperature (t) during the study period.

urea hydrolysis and diffusion restrict NH_3 release, while at high water content, dilution and reduced gas diffusion suppress volatilization. Maximum emissions typically occur at intermediate moisture (~50% VWC), when hydrolysis, diffusion, and evaporation are optimally balanced (Ren et al., 2023). In a broader context, soil and surface moisture also influence the bidirectional NH_3 exchange by modifying surface resistance and the canopy compensation point (Sutton et al., 2013). Episodes of rainfall (Fig. 3) also contributed to transient increases, as they enhanced NH_4^+ availability at the soil surface. However, fluxes decreased rapidly under cooler or drier intervals, indicating a strong short-term control by microclimatic conditions. Overall, NH_3 flux responded most directly and strongly to fertilizer application and subsequent meteorological conditions, with clear peaks aligned with warm and moist periods.

3.3. Machine-learning analysis

3.3.1. NH_3 flux – relationships with environmental variables

Across both validation schemes, RF achieved the highest predictive accuracy among all models (Table 3). Linear baselines (OLS, Ridge, Lasso, PLSR) yielded markedly lower R^2 and substantially higher errors, indicating that they failed to capture the non-linearities and interactions that characterize soil-plant-atmosphere exchange processes. With 360 observations and eight predictors, the 500-tree RF ensemble provided sufficient flexibility to represent complex responses, while averaging across trees helped stabilize predictions within the range of the observed data. Model predictions vs. measurements for the RF (Fig. 4) show a near-1:1 relationship with moderate dispersion, consistent with the CV accuracy range and indicating reasonable predictive agreement within the present dataset.

It should be noted that model performance may have been influenced by repeated measurements at the same sampling locations, which introduced some degree of dependency among observations. Consequently, the model results should be interpreted primarily in terms of relative variability and driver–response relationships rather than as fully independent estimates of predictive performance. However, the strong performance of Random Forest is consistent with its ability to capture complex, non-linear relationships in environmental datasets. We also compared RF models trained with 500 versus 1000 trees. The overall predictive performance and variance explanation remained highly consistent between the two configurations (R^2 varied only from 0.767 to 0.773), with only minor differences in the fit. The slightly smoother alignment of the 1000-tree predictions reflects reduced variance from averaging over a larger ensemble, but the gain in accuracy beyond 500 trees was marginal, indicating that model performance had essentially converged. For this reason, the RF with 500 trees was retained as the reference model for interpretation and prediction.

Feature-importance rankings differed between the two approaches. Impurity-based Random Forest feature importance ranked Γ highest, followed by soil temperature and VWC, whereas mean absolute SHAP importance produced a somewhat different ranking (Fig. 5). This divergence is expected because the two approaches quantify different aspects of predictor relevance, and correlations among predictors can redistribute importance or attribution in both methods. Moreover, both measures quantify the magnitude rather than the direction of predictor

Table 3
Performance metrics from 10-fold KFold cross-validation.

Model	R^2 mean	R^2 SD	RMSE Mean	RMSE SD	MAE Mean	MAE SD
Random Forest	0.739	0.136	2.708	0.818	1.723	0.415
Lasso	0.051	0.157	5.430	1.119	3.810	0.335
Ridge	0.037	0.175	5.458	1.083	3.856	0.316
PLSR	0.037	0.174	5.459	1.085	3.857	0.321
OLS	0.036	0.176	5.459	1.082	3.858	0.315

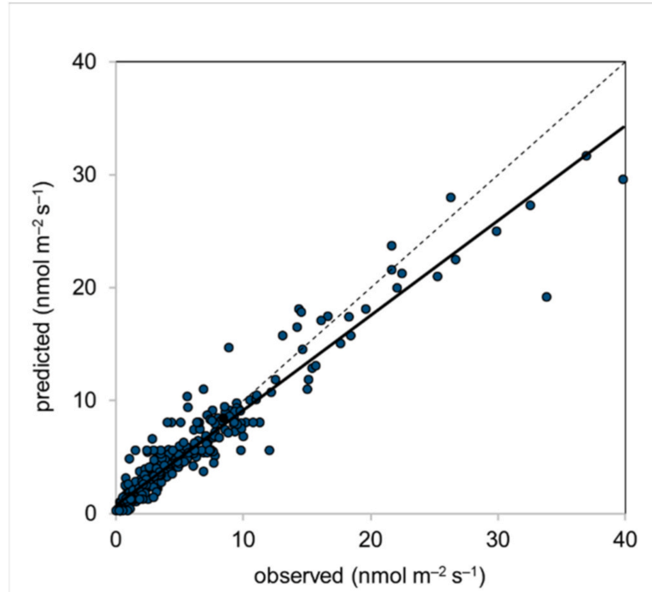

Fig. 4. Measured vs. predicted NH_3 flux (RF, single split).

contributions. Their rankings should therefore be interpreted as complementary model-based associations rather than as evidence of independent or causal effects.

These leading predictors are consistent with mechanistic understanding. Soil temperature and VWC regulate both microbial kinetics and diffusive transport of NH_3/NH_4^+, producing strong, often non-linear responses (Ren et al., 2023). Humus also appears among the key predictors, consistent with its influence on soil buffering capacity, sorption, and the stabilization of ammoniacal N pools. Γ reflects the soil NH_3 compensation point concentration, defined by the molar ratio of NH_4^+ to H^+ ions in soil solution, and thus represents volatilization potential (Sutton et al., 1994). Although NO_3^- ranked moderately high, NH_3 volatilization is primarily governed by ammoniacal N and pH rather than nitrate per se (Ren et al., 2023), so its importance likely reflects covariation or indirect pathways. This model-derived association is examined more cautiously in Section 3.3.3. Total N played a smaller role, while canopy structure (hc, LAI) contributed negligibly, consistent with periods when soil-surface exchange dominates within a bidirectional resistance framework (Sutton et al., 2013).

Multiple field, lab, and modeling studies identify soil wetness (VWC) as a primary control on NH_3 volatilization, often with a characteristic unimodal ("dome-shaped") response. Under dry conditions, dissolution and hydrolysis of urea-based fertilizers are water-limited, suppressing NH_3 formation; at intermediate VWC, dissolution, hydrolysis, and gas transport are simultaneously efficient, yielding peak emissions; at high VWC, gaseous NH_3 diffusion is impeded and a larger fraction remains in solution or is leached downward, damping volatilization. The timing of rainfall/irrigation relative to fertilizer application thus critically modulates losses (Black et al., 1987; Farooq et al., 2024; Frößl et al., 2025; Hurtado et al., 2024). This mechanistic picture is consistent with the bidirectional exchange/compensation-point framework in which NH_3 exchange depends on surface microlayer chemistry (e.g. Γ) and conductance that vary with moisture (Flechard et al., 2013; Nemitz et al., 2001; Massad et al., 2010). Recent process-model and ML analyses likewise elevate moisture among the top predictors of NH_3 loss and related N fluxes across climates and crops (Frößl et al., 2025; Hurtado et al., 2024; Jiang et al., 2024).

Γ directly captures the pH-dependent equilibrium of NH_3/NH_4^+ partitioning: at higher Γ (higher NH_4^+ and/or lower H^+), the gas-phase fraction of NH_3 increases in the surface micro-environment, and rising Γ directly strengthens volatilization. The interaction between Γ and

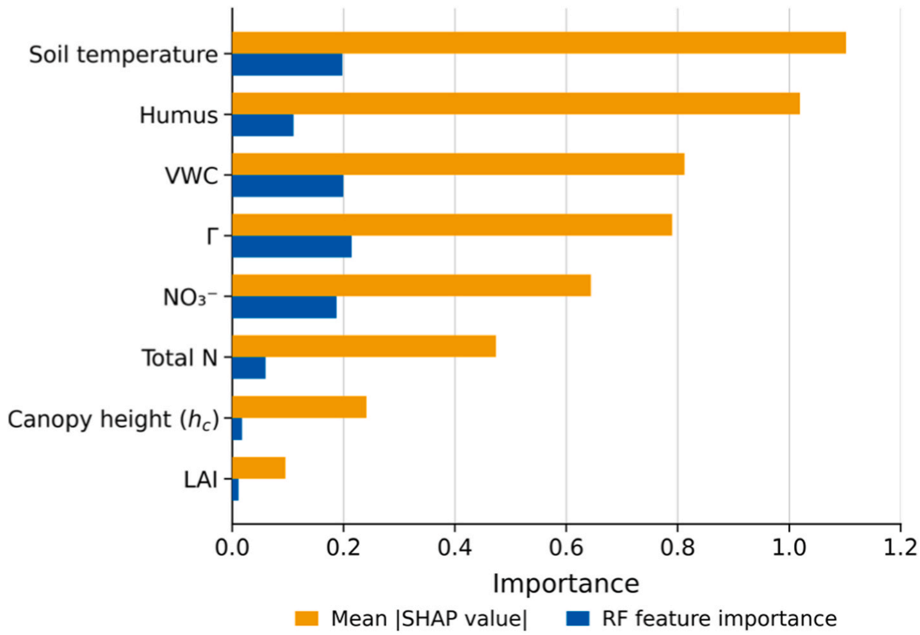

Fig. 5. Comparison of cross-validated Random Forest feature importance and mean absolute SHAP importance derived from the single-split RF model. Both measures quantify the magnitude of predictor importance but do not indicate whether individual predictors increase or decrease the predicted NH_3 flux.

VWC is crucial: the chemical driving force can only fully express itself if VWC still allows gas transport (Flechard et al., 2013; Massad et al., 2010; Nemitz et al., 2001). Temperature further accelerates urease activity, raises the pH of the surface micro-zone, and reduces NH_3 solubility, thereby shifting the equilibrium toward the gas phase while steepening the soil-atmosphere concentration gradient. The effect of temperature is typically conditional and is amplified in combination with VWC and Γ; warm, moderately moist conditions thus pose the highest risk (Flechard et al., 2013; Massad et al., 2010).

The results are therefore consistent with a broader body of experimental and modeling work. In fertilized systems, RF applied to large, heterogeneous field datasets has successfully identified the main drivers of NH_3 volatilization; in Mediterranean climates, for example, soil pH and N rate emerged as key factors, and RF performed well in predicting the emission factor (EF) and cumulative losses (Hurtado et al., 2024). In a recent comparative study, RF and other ML models evaluated NH_3 emissions from slurry/manure experiments, where ML approaches consistently outperformed simpler empirical methods and provided tractable variable-importance and partial-dependence (PDP/SHAP) insights into VWC-temperature-pH-management interactions (Favrot et al., 2025).

Based on the joint picture of the leading predictors (temperature, humus, VWC, Γ, NO_3^-), mitigating NH_3 loss emerges as a state-dependent optimization problem: (i) control VWC via post-application water management and/or incorporation; (ii) reduce Γ by limiting surface pH rise and using urease inhibitors; (iii) avoid warm, dry, windy periods for surface urea application; and (iv) regulate the rate of nitrification through inhibitors and dose/timing management (Cantarella et al., 2018; Flechard et al., 2013; Sutton et al., 2013).

Overall, the comparison of modeling approaches underscores the limitations of linear regression, penalized regression (Ridge, Lasso), and PLSR for NH_3 flux prediction in this data set. These approaches failed to capture the non-linearities and interactions governing soil-plant-atmosphere exchange. By contrast, RF effectively exploited such interactions, explaining a large fraction of the variance and achieving substantially lower error metrics than linear alternatives. This strong alignment between statistical importance and biogeochemical reasoning strengthens confidence in the robustness of the RF results. Beyond predictive accuracy, RF models provide practical interpretability through partial dependence profiles, which can visualize marginal effects and communicate mechanistic plausibility to a wider audience.

Despite its strong predictive performance, RF also has important limitations. Unlike conventional regression models, RF does not provide an explicit equation relating the predictors to NH_3 flux and therefore functions largely as a black-box model. Although feature-importance measures, SHAP values, and partial dependence plots can improve interpretation, they do not convert modelled associations into causal relationships. Moreover, RF predictions are generally most reliable within the range of environmental and soil conditions represented in the training data. Because tree-based models have limited capacity to extrapolate beyond the observed predictor ranges, their predictions may become unreliable under substantially different climatic, soil, crop, or fertilization conditions. Consequently, the present model should primarily be regarded as a tool for identifying nonlinear relationships and generating hypotheses within the conditions covered by this dataset; its broader applicability requires validation using independent observations from other sites, seasons, and management systems.

3.3.2. Soil depth effects on NH_3 flux

To assess depth-resolved soil controls on NH_3 flux, we examined the layer-specific contributions of Γ, total N, NO_3^-, and humus across the 0–10, 10–20, and 20–30 cm soil layers. Only predictors measured separately at all three depths were included. Therefore, unlike the analysis presented in Section 3.3.1, this analysis did not include VWC, soil temperature, LAI, or canopy height. The modeling and validation procedures followed those described in Section 2.6.

The Random Forest model substantially outperformed all linear approaches and achieved a mean R^2 of 0.690 with low prediction errors

Table 4
Performance metrics from 10-fold KFold cross-validation.

Model	R^2 mean	R^2 SD	RMSE Mean	RMSE SD	MAE Mean	MAE SD
Random Forest	0.690	0.130	3.041	0.817	1.825	0.369
Lasso	0.055	0.082	5.471	1.264	3.803	0.496
Ridge	0.049	0.072	5.498	1.294	3.783	0.533
PLSR	0.039	0.082	5.515	1.259	3.801	0.531
OLS	0.048	0.072	5.501	1.296	3.783	0.534

(Table 4). Linear models performed consistently poorly ($R^2 < 0.05$), suggesting that the observed NH_3 flux variability involved non-linear and depth-dependent relationships that were not adequately represented by the tested linear models. Random Forest variable importance identified humus content in the 0–10 cm layer and gamma at 20–30 cm and 10–20 cm as the most influential predictors (Fig. 6).

The SHAP analysis provided a more nuanced picture, highlighting similarly strong contributions from humus (0–10 cm), nitrate and total N concentrations, gamma, and humus at 20–30 cm depth. These variables showed the highest average absolute SHAP values, indicating that both organic matter availability and inorganic nitrogen status, across shallow and deeper layers, substantially shaped NH_3 emission predictions. However, their positive or negative effects cannot be inferred from the importance values shown in Fig. 6.

These results indicate that properties of both shallow and deeper soil layers contributed to the modelled variation in NH_3 flux. The recurring model importance of variables measured at 20–30 cm suggests an association between NH_3 flux variability and vertically structured soil conditions. However, feature importance alone does not establish that processes occurring at this depth directly regulated surface NH_3. Overall, the modeling results indicate that NH_3 flux variability was associated with a combination of organic matter availability, soil nitrogen status, and soil physical properties across the soil profile. The better predictive performance of the Random Forest model relative to the tested linear models suggests that non-linear relationships and interactions contributed to the observed NH_3 flux variability. SHAP analysis provided model-specific estimates of the relative contribution of individual predictors. Together, these findings highlight the value of machine-learning approaches for disentangling the multifaceted drivers of gaseous nitrogen losses under field conditions.

Previous studies have also highlighted that the vertical distribution of nitrogen and the depth of nitrogen transformations strongly modulate NH_3 volatilization, even if they did not explicitly analyze the same set of depth-stratified predictors as in our study. Field and incubation experiments consistently show that the majority of NH_3 losses arise when urea or ammonium fertilizers remain near the soil surface (0-5 cm), whereas deeper placement markedly reduces emissions. For example, Rochette et al. (2013) found that banding urea at increasing depths from the surface down to 10 cm led to a strong, non-linear decline in NH_3 losses, with near-surface placement producing the highest emissions. Pan et al. (2016) and Zhong et al. (2021) similarly reported that subsurface banding or deep placement of N fertilizers reduced volatilization by roughly 50-80% compared with surface broadcasting, while also improving nitrogen use efficiency. More recent work by Götze et al. (2023) and Zhou et al. (2022) confirmed that deep incorporation or slit injection at around 10 cm depth can reduce NH_3 emissions by >70% relative to standard surface application. In pot and field experiments, Liu et al. (2015) and Xiang et al. (2013) showed that placing N at 5-10 cm depth substantially decreases NH_3 loss compared with surface application, again pointing to a strong vertical gradient in emission potential.

Although these studies focus mainly on fertilizer placement depth rather than depth-resolved soil properties, they all imply that NH_3 production and release are highly sensitive to how close reactive N is to the soil-air interface. Modeling work on NO and N_2O further supports this concept: when the depth of gas production was shifted from 0–10 cm to 10–20 cm, surface NO flux decreased to only ~1% of its original value, while N_2O flux changed much less, underlining the critical role of production depth in determining emission rates (Hosen et al., 2000). Taken together, these findings are consistent with our results, which indicate that while surface humus content exerts a strong control on NH_3 emissions, subsoil layers (particularly 20–30 cm) also play an important role via their inorganic N pools and physical properties. In other words, our depth-resolved analysis of humus, NO_3^-, total N and gamma refines and extends earlier evidence that NH_3 volatilization emerges from vertically structured interactions between near-surface N availability and subsoil conditions governing gas

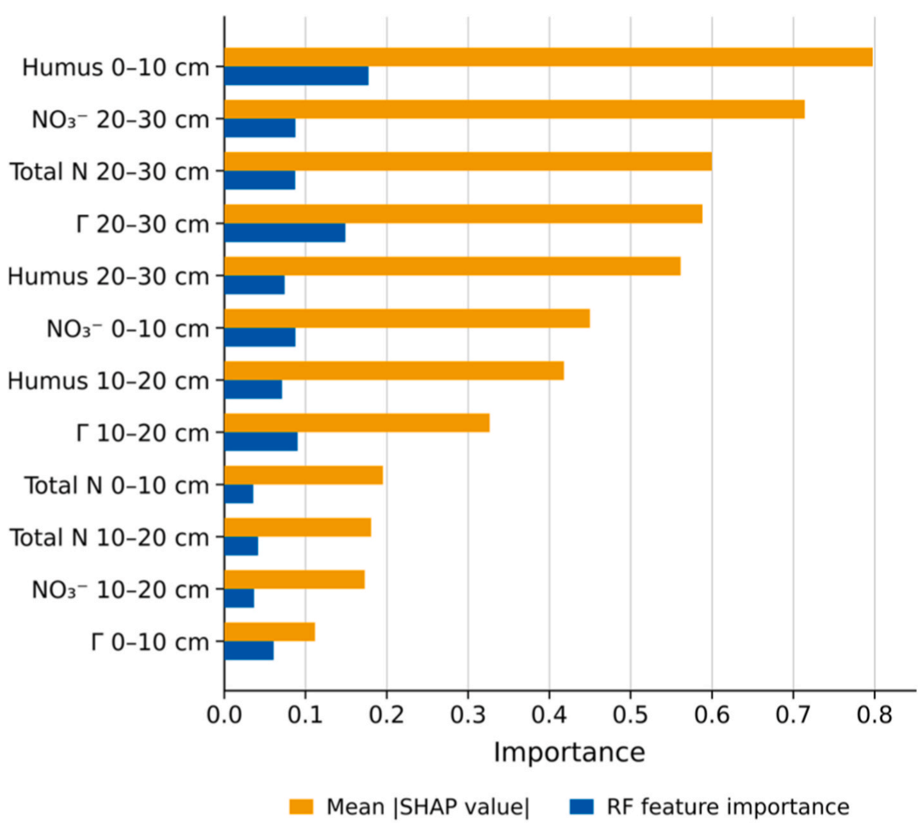

Fig. 6. Comparison of cross-validated Random Forest feature importance and mean absolute SHAP importance for the depth-resolved model. Both measures quantify the magnitude of predictor importance but do not indicate the direction of predictor effects on the predicted NH_3 flux.

diffusion and nitrogen transformation.

An additional mechanism potentially contributing to the observed depth-dependent relationships is the vertical stratification of soil microbial communities. Microbial biomass, community composition, and the abundance and activity of functional groups involved in N cycling commonly vary with soil depth (Eilers et al., 2012). In particular, ammonification, microbial NH_4^+ immobilization, and ammonia oxidation by ammonia-oxidizing bacteria and archaea regulate the size and persistence of the soil NH_4^+ pool (Di et al., 2009). Nitrification can additionally decrease microsite pH through proton production, thereby shifting the NH_4^+/NH_3 equilibrium towards the non-volatile ionic form. Consequently, differences in microbial communities among soil layers may partly underlie the depth-specific associations of humus, NO_3^-, total N, and Γ with surface NH_3 flux. The measured physicochemical predictors may therefore also act as indirect proxies for unmeasured microbial processes. Nevertheless, because microbial biomass, community composition, functional-gene abundance, and N-transformation rates were not determined in this study, the contribution of microbial stratification cannot be separated from that of the measured physicochemical gradients. Future studies combining depth-resolved soil analyses with microbial community profiling and direct measurements of ammonification and nitrification would be required to test this mechanism.

3.3.3. Modelled associations between NO_3^- and NH_3 flux

NO_3^- emerged as a relatively important predictor in the RF analysis; however, this result should not be interpreted as evidence of a direct causal effect on NH_3 volatilization. Unlike NH_4^+ and pH, which directly determine the NH_4^+/NH_3 equilibrium and are represented jointly by Γ, NO_3^- is not a direct substrate for NH_3 production. Its model importance may instead reflect covariance with NH_4^+ availability, fertilizer input, nitrification progress, soil moisture, temperature, or other unmeasured N-transformation processes. Because correlated predictors can share or redistribute importance in RF, SHAP, permutation-importance, and partial-dependence analyses, the independent contribution of NO_3^- cannot be isolated from the present observational dataset. NO_3^- should therefore be regarded as an indicator of the soil N-transformation state rather than as a direct regulator of NH_3 loss.

The relatively modest contribution of measured NH_4^+ and the comparatively greater importance of NO_3^- should be interpreted with caution because the soil samples were air-dried before chemical analysis. Air drying can cause partial loss of ammoniacal N, particularly from soils with high initial NH_4^+ concentrations and elevated pH (Rochester et al., 1991). Although all samples underwent the same analytical protocol, the magnitude of this loss may not have been identical among samples and could have attenuated the observed NH_4^+ variability. This potential artifact may also have affected the Γ proxy because measured NH_4^+ was used in its calculation. Consequently, the model results should not be interpreted as evidence that NO_3^- is intrinsically a stronger causal regulator of NH_3 volatilization than NH_4^+. Rather, NO_3^- should be regarded as a depth- and state-dependent indicator of broader N-transformation dynamics, while the relatively low importance of measured NH_4^+ may partly reflect sample preparation.

Previous studies have likewise reported contrasting associations between soil NO_3^- and NH_3 volatilization. Wan et al. (2024) reported that soil NO_3^- content may be associated with enhanced NH_3 emissions, whereas Feng et al. (2022) identified increased NO_3^-concentration and soil cation-exchange capacity as important contributors to reduced NH_3 volatilization. These contrasting observations further indicate that NO_3^- primarily reflects context-dependent soil N-transformation processes, including nitrification and denitrification, rather than a uniform direct effect on NH_3 loss (Cameron et al., 2013; Ju et al., 2009).

Partial dependence plots (PDPs) were computed for NO_3^- both in one dimension (stratified by depth) and in two dimensions (joint effects with VWC and soil temperature). For visualization, predictor values were displayed on standardized scales and restricted to their observed ranges, while partial dependence was presented on a relative model-output scale to facilitate comparison among panels. Among all modeling approaches tested, the Random Forest (RF) regression achieved the best predictive performance for NH_3 flux, outperforming linear (OLS, Ridge, Lasso) and latent-factor (PLSR) methods. The better predictive performance of RF suggests that non-linear relationships and possible predictor interactions contributed to the observed flux variability and were represented more effectively by RF than by the tested linear models. RF also reproduced threshold-type behaviors in soil moisture and temperature and proved more robust to collinearity among environmental predictors.

Depth-specific patterns are illustrated by the 1D PDP stratified by soil depth (Fig. 7a). The NO_3^- effect varied distinctly among the 0–10, 10–20, and 20–30 cm layers, indicating that NO_3^-–NH_3 relationships are depth-dependent. This likely reflects vertical gradients in redox potential, substrate availability, and microbial activity. At shallower depths, NO_3^- accumulation may enhance microbial turnover and indirectly favor NH_3 release, whereas at deeper layers, lower aeration and higher moisture constrain volatilization even at comparable NO_3^- levels. These findings underscore the heterogeneity of soil microenvironments and the limitations of bulk-layer correlations.

Moisture interactions are illustrated by the 2D PDP for NO_3^- versus VWC (Fig. 7b). NH_3 emissions increased markedly under high VWC conditions across most of the NO_3^-gradient, indicating that wet soils promoted volatilization in our dataset. Under drier conditions, NO_3^- had little influence, suggesting that water limitation curtailed microbial activity and diffusion despite sufficient aeration. Conversely, in wetter soils, even modest NO_3^- concentrations coincided with elevated fluxes, potentially reflecting intensified microbial activity and reduced NH_3 re-uptake under near-anaerobic microsites. Such behavior implies that different microbial pathways dominate across the NO_3^- gradient: at low NO_3^-, reduced conditions (e.g. denitrification) may prevail, maintaining higher local pH through weaker proton production; at intermediate NO_3^-, active nitrification acidifies microsites and suppresses NH_3 release; and at high NO_3^-, fertilizer co-variation or enhanced microbial metabolism again favors volatilization. These context-dependent responses are consistent with moisture-mediated controls observed by Ju et al. (2009), Di et al. (2009), and Götze et al. (2023). These relationships should be interpreted as model-derived associations rather than causal effects.

Temperature interactions are shown by the 2D PDP for NO_3^- versus soil temperature (Fig. 7c). The strongest NH_3 fluxes occurred under cooler soils with low NO_3^- levels. Reduced microbial activity under low temperature limits nitrification and proton generation, allowing carbonate buffering to sustain relatively high pH and thus favor volatilization. Moreover, at low temperatures, NH_4^+ oxidation, microbial immobilization, and cation exchange proceed slowly, prolonging the availability of NH_4^+ in the soil solution (Jones et al., 2013). In contrast, under warmer conditions, nitrification accelerates, producing protons that acidify microsites and shift the NH_4^+/NH_3 equilibrium toward NH_4^+, suppressing volatilization. This pattern aligns with the RF predictor importance, where temperature ranked as the single strongest driver of NH_3 flux, yet its effect was clearly modulated by NO_3^- availability. Although higher temperatures typically promote volatilization potential (Fenn and Kissel, 1974; Sommer et al., 2004), this effect can be counteracted under NO_3^--rich conditions through nitrification-induced acidification.

Collectively, the PDPs reveal nonlinear, context-dependent associations between measured NO_3^- and predicted NH_3 flux across soil depths, moisture conditions, and temperatures. However, these patterns do not demonstrate that NO_3^- directly regulates NH_3 volatilization. They may reflect covariance with NH_4^+ availability, fertilizer history, nitrification, environmental conditions, or unmeasured microbial processes. PDPs also average predictions across the distributions of other predictors and should be interpreted cautiously when predictors are correlated. Possible underestimation of NH_4^+ following air drying may additionally have increased the apparent relative importance of NO_3^-. Accordingly, these results should be regarded as hypothesis-generating associations

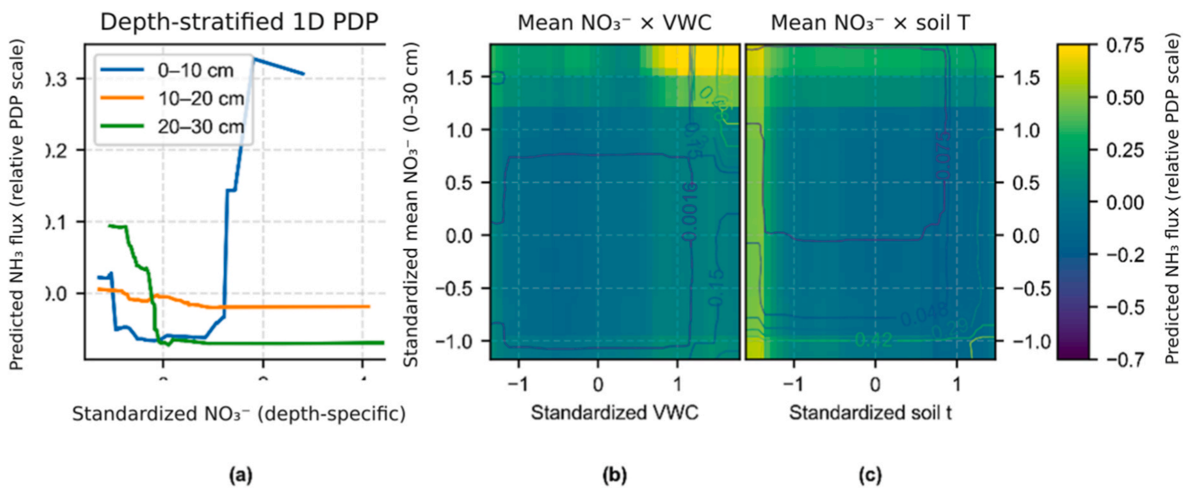

Fig. 7. Partial dependence plots illustrating the modelled associations between NO_3^- and predicted NH_3 flux. (a) Depth-specific one-dimensional PDPs for NO_3^- at 0–10, 10–20, and 20–30 cm, obtained from the depth-resolved RF model. (b) Two-dimensional PDP for depth-averaged NO_3^- and VWC, obtained from the primary RF model. (c) Two-dimensional PDP for depth-averaged NO_3^- and soil temperature, obtained from the primary RF model. Predictor values are shown on the standardized scale. PDPs represent model-derived associations and should not be interpreted as causal effects.

rather than evidence of a direct causal mechanism.

From a management standpoint, NH_3 losses from ammonium nitrate fertilizers are not fixed but strongly modulated by soil conditions. Avoiding fertilizer exposure under dry, alkaline conditions and aligning applications with rainfall or incorporation can significantly reduce volatilization (Al-Kanani et al., 1991; Black et al., 1987; Rochette et al., 2009; Sommer et al., 2004). However, nitrification-driven acidification entails trade-offs: while it suppresses NH_3 losses, it may simultaneously enhance N_2O emissions and NO_3^- leaching. Meta-analyses show that nitrification inhibitors mitigate N_2O and leaching but can elevate NH_3 volatilization (Rochette et al., 2009, 2013; Qiao et al., 2015), underscoring the multidimensional nature of nitrogen management.

4. Conclusion

This study indicates that NH_3 flux variability in fertilized cropland is associated with complex, non-linear relationships among soil chemical properties, microclimatic conditions, and vertical soil heterogeneity. Machine-learning analysis, particularly Random Forest combined with SHAP interpretation, identified the leading model predictors associated with NH_3 flux variability. A limitation of the study is the absence of an unfertilized control treatment, which restricts the direct quantification of fertilizer-induced NH_3 emission increments. However, the focus of this study was on within-field variability and environmental controls rather than treatment comparison. Soil temperature, moisture, humus content, and the NH_4^+/H^+ proxy (Γ) emerged as leading model predictors. Properties measured at 20–30 cm also contributed to the predictions, indicating an association between NH_3 flux variability and vertically structured soil conditions rather than surface properties alone. NO_3^- emerged as a conditional, state-dependent model predictor, but this association should be interpreted as an indicator of broader N-transformation dynamics rather than as evidence of a direct causal effect on NH_3 volatilization.

A limitation of the study is that flux measurements were conducted at discrete time points, which may not fully capture short-term emission peaks or diurnal variability. Consequently, cumulative emission estimates should be interpreted as approximate. However, the primary objective of this work was not to derive a complete emission budget, but to identify the key environmental controls of NH_3 flux.

Overall, the findings indicate that machine-learning approaches applied to multi-point field datasets can help identify complex associations between environmental variables and NH_3 fluxes and can support the development of hypotheses concerning the underlying processes. These findings suggest that the possible contribution of subsurface N dynamics warrants further investigation when developing NH_3 mitigation strategies.

CRediT authorship contribution statement

Eszter Tóth: Writing – review & editing, Methodology, Investigation, Conceptualization. **János Balogh:** Writing – review & editing, Methodology, Investigation. **Zoltán Bozóki:** Funding acquisition, Data curation. **László Horváth:** Writing – original draft, Methodology, Investigation, Conceptualization. **Zoltán Nagy:** Writing – review & editing, Funding acquisition, Data curation. **Zsófia Oltvári:** Software, Methodology. **Tünde Takács:** Writing – review & editing, Investigation. **Krisztina Pintér:** Writing – review & editing, Methodology, Investigation.

Data availability

Data will be made available on request.

Declaration of generative AI and AI-assisted technologies in the manuscript preparation process

During the preparation of this work, the authors used ChatGPT (OpenAI, GPT-5) to assist in exploring methodological options and structuring the modeling approach applied in the study. After using this tool, the authors critically evaluated all AI-generated suggestions, performed the analyses independently, and take full responsibility for the design, implementation, and interpretation of the research and for the content of the published article.

Funding

The research was funded by the Sustainable Development and Technologies National Programme of the Hungarian Academy of Sciences (FFT NP FTA), and by the Hungarian Research and Technology Innovation Fund (OTKA), project no. K-138176. Investigations were supported by the János Bolyai Research Scholarship of the Hungarian Academy of Sciences (grant no. BO/00548/23).

Declaration of competing interest

The authors declare that they have no known competing financial interests or personal relationships that could have appeared to influence the work reported in this paper.

Acknowledgements

Special thanks to Péter Ecker for technical support.

Appendix A. Supplementary data

Supplementary data to this article can be found online at https://doi.org/10.1016/j.apr.2026.103202.

References

Adjuik, T.A., Davis, S.C., 2022. Machine learning approach to simulate soil CO_2 fluxes under cropping systems. Agronomy 12, 197. https://doi.org/10.3390/agronomy12010197.
Al-Kanani, T., MacKenzie, A.F., Barthakur, N.N., 1991. Soil water, ammonia volatilization relationships with surface-applied nitrogen fertilizer solutions. Soil Sci. Soc. Am. J. 55, 1761–1766.
Andrade, C., 2021. Z scores, standard scores, and composite test scores explained. Indian J. Psychol. Med. 43, 555–557. https://doi.org/10.1177/02537176211046525.
Bindraban, P.S., Dimkpa, C.O., White, J.C., Franklin, F.A., Melse-Boonstra, A., Koele, N., 2020. Safeguarding human, planetary health demands a fertilizer sector transformation. Plants People Planet 2, 302–309.
Black, A.S., Sherlock, R.R., Smith, N.P., 1987. Effect of timing of simulated rainfall on ammonia volatilization from urea, applied to soil of varying moisture content. J. Soil Sci. 38, 679–687.
Bouwman, A.F., Boumans, L.J.M., Batjes, N.H., 2002. Estimation of global NH_3 volatilization loss from synthetic fertilizers and animal manure applied to arable lands and grasslands. Glob. Biogeochem. Cycles 16, 1024. https://doi.org/10.1029/2000GB001389.
Bremner, J.M., Keeney, D.R., 1966. Determination and isotope-ratio analysis of different forms of nitrogen in soils: 3 exchangeable ammonium, nitrate, and nitrite by extraction-distillation methods. Soil Sci. Soc. Am. J. 30, 577–582. https://doi.org/10.2136/sssaj1966.03615995003000050015x.
Bussink, D.W., 1994. Relationships between ammonia volatilization and nitrogen fertilizer application rate, intake and excretion of herbage nitrogen by cattle on grazed swards. Fert. Res. 38, 111–121.
Butterbach-Bahl, K., Baggs, E.M., Dannenmann, M., Kiese, R., Zechmeister-Boltenstern, S., 2013. Nitrous oxide emissions from soils: how well do we understand the processes, their controls? Philos. Trans. R. Soc. B 368, 20130122.
Cameron, K.C., Di, H.J., Moir, J.L., 2013. Nitrogen losses from the soil/plant system: a review. Ann. Appl. Biol. 162, 145–173.
Canatoy, R.C., Cho, S.R., Galgo, S.J.C., Kim, P.J., Kim, G.W., 2024. Reducing ammonia volatilization in rice paddy: the importance of lower fertilizer rates, soil incorporation. Front. Environ. Sci. 12, 1479712. https://doi.org/10.3389/fenvs.2024.1479712.
Cantarella, H., Otto, R., Soares, J.R., de Brito Silva, A.G., 2018. Agronomic efficiency of NBPT as a urease inhibitor: a review. J. Adv. Res. 13, 19–27.
Chae, H.G., Song, H.J., Bhuiyan, M.S.I., Kim, P.J., Lee, J.G., 2022. Unexpected high suppression of ammonia volatilization loss by plastic film mulching in Korean maize cropping system. Agric. Ecosyst. Environ. 335, 108022.
Coskun, D., Britto, D.T., Shi, W., Kronzucker, H.J., 2017. Nitrogen transformations in modern agriculture, the role of biological nitrification inhibition. Nat. Plants 3, 1–10.
Deng, X., Xu, T., Xue, L., Hou, P., Xue, L., Yang, L., 2023. Effects of warming, fertilization on paddy N_2O emissions, ammonia volatilization. Agric. Ecosyst. Environ. 347, 108361.
Dhaliwal, J.K., Panday, D., Robertson, G.P., Saha, D., 2025. Machine learning reveals dynamic controls of soil nitrous oxide emissions from diverse long-term cropping systems. J. Environ. Qual. 54, 132–146. https://doi.org/10.1002/jeq2.20637.
Di, H.J., Cameron, K.C., Shen, J.P., Winefield, C.S., O'Callaghan, M., Bowatte, S., He, J.Z., 2009. Nitrification driven by bacteria, not archaea in nitrogen-rich grassland soils. Nat. Geosci. 2, 621–624.
Eilers, K.G., Debenport, S., Anderson, S., Fierer, N., 2012. Digging deeper to find unique microbial communities: the strong effect of depth on the structure of bacterial and archaeal communities in soil. Soil Biol. Biochem. 50, 58–65. https://doi.org/10.1016/j.soilbio.2012.03.011.
FAO (2020), 2020. Standard Operating Procedure for Soil Organic Carbon, Walkley-Black Method, Titration and Colorimetric Method. FAO, Rome, Italy. https://www.fao.org/3/ca7471en/ca7471en.pdf.
Farooq, M.S., Mahmood, R., Hameed, A., Ali, S., Nadeem, F., Awan, T.H., Fatima, A., Ahmad, Z., 2024. Optimizing nitrogen sources in top dressing for wheat: field Study on growth, yield, and ammonia volatilization. Sci. Tech. Rep. 2024, 8882675.
Farquhar, G.D., Firth, P.M., Wetselaar, R., Weir, B., 1980. On the gaseous exchange of ammonia between leaves, the environment: determination of the ammonia compensation point. Plant Physiol. 66, 710–714.
Favrot, A., Génermont, S., Décuq, C., Makowski, D., 2025. Machine learning for ammonia volatilization prediction and slurry application management. J Environ Sci 160, 481–489. https://doi.org/10.1016/j.jes.2025.04.045.
Feng, Y., Han, L., Sun, H., Zhu, D., Xue, L., Jiang, Z.T., Poinern, G.E.J., Lu, Q., Feng, Y., Xing, B., 2022. Every coin has two sides: continuous, substantial reduction of ammonia volatilization under the coexistence of microplastics. biochar in an annual observation of rice-wheat rotation system Sci Total Environ 847, 157635.
Fenn, L.B., Kissel, D.E., 1974. Ammonia volatilization from surface applications of ammonium compounds on calcareous soils: i effects of temperature, rate of ammonium nitrogen application. Soil Sci. Soc. Am. J. 38, 606–610.
Fisher, A., Rudin, C., Dominici, F., 2019. All models are wrong, but many are useful: learning a variable's importance by studying an entire class of prediction models simultaneously. J. Mach. Learn. Res. 20, 1–81.
Flechard, C.R., Massad, R.-S., Loubet, B., Personne, E., Simpson, D., Bash, J.O., Cooter, E. J., Nemitz, E., Sutton, M.A., 2013. Advances in understanding, models and parameterizations of biosphere–atmosphere ammonia exchange. Biogeosciences 10, 5183–5225.
Forrestal, P.J., Harty, M., Carolan, R., Lanigan, G.J., Watson, C.J., Laughlin, R.J., McNeill, G., Chamber, N.J., Richards, K.G., 2016. Ammonia emissions from urea, stabilized urea, calcium ammonium nitrate: insights into loss abatement in temperate grassland. Soil Use Manage. 32, 92–100. https://doi.org/10.1111/sum.12232.
Fritsch, F.N., Butland, J., 1984. A method for constructing local monotone piecewise cubic interpolants SIAM. J Sci Stat Comput 5, 300–304.
Fritsch, F.N., Carlson, R.E., 1980. Monotone piecewise cubic interpolation SIAM. J Numer Anal 17, 238–246.
Frößl, J., Scholl, M., Hartung, J., Ruser, R., Müller, T., 2025. How do soil moisture and simulated rainfall drive ammonia emissions after applying inhibited urea fertilizers?–An incubation study. J. Environ. Manag. 376, 124435.
Galloway, J.N., Aber, J.D., Erisman, J.W., Seitzinger, S.P., Howarth, R.W., Cowling, E.B., Cosby, B.J., 2003. The nitrogen cascade. Bioscience 53, 341–356.
Gan, C., Jiang, Y., Wang, Y., Lin, S., Hu, R., 2025. Organic fertilizer application reduces ammonia volatilization in an acidic soil. Agric. Ecosyst. Environ. 383, 109510. https://doi.org/10.1016/j.agee.2025.109510.
Génermont, S., Cellier, P., 1997. A mechanistic model for estimating ammonia volatilization from slurry applied to bare soil. Agric. For. Meteorol. 88, 145–167.
Götze, H., Saul, M., Jiang, Y., Pacholski, A., 2023. Effect of incorporation techniques, soil properties on NH_3, N_2O emissions after urea application. Agronomy 13, 2632.
He, Z.L., Alva, A.K., Calvert, D.V., Banks, D.J., 1999. Ammonia volatilization from different fertilizer sources, effects of temperature, soil pH. Soil Sci. 164, 750–758.
Horváth, L., Asztalos, M., Führer, E., Mészáros, R., Weidinger, T., 2005. Measurement of ammonia exchange over grassland in the Hungarian Great Plain. Agric. For. Meteorol. 130, 282–298.
Hosen, Y., Tsuruta, H., Minami, K., 2000. Effects of the depth of NO and N_2O productions in soil on their emission rates to the atmosphere: analysis by a simulation model. Nutrient Cycl. Agroecosyst. 57, 83–98.
Hurtado, J., Velázquez, E., Lassaletta, L., Guardia, G., Aguilera, E., Sanz-Cobena, A., 2024. Drivers of ammonia volatilization in Mediterranean climate cropping systems. Environ. Pollut. 341, 122814.
ISO, 1995. ISO 11261:1995 Soil Quality - Determination of Total Nitrogen - Modified Kjeldahl Method. International Organization for Standardization, Geneva, Switzerland.
IUSS Working Group WRB, 2022. World Reference Base for Soil Resources: International Soil Classification System for Naming Soils and Creating Legends for Soil Maps, fourth ed. International Union of Soil Sci (IUSS).
Jiang, J., Feng, L., Hu, J., Liu, H., Zhu, C., Chen, B., Chen, T., 2024. Global soil respiration predictions with associated uncertainties from different spatio-temporal data subsets. Ecol. Inform. 82, 102777.
Jiang, Y., Deng, A., Bloszies, S., Huang, S., Zhang, W., 2017. Nonlinear response of soil ammonia emissions to fertilizer nitrogen. Biol. Fertil. Soils 53, 269–274.
Jones, C., Brown, B.D., Engel, R., Horneck, D., Olson-Rutz, K., 2013. Nitrogen Fertilizer Volatilization. Montana State University Extension. EBO208.
Ju, X.T., Xing, G.X., Chen, X.P., Zhang, S.L., Zhang, L.J., Liu, X.J., Cui, Z.L., Yin, B., Christie, P., Zhu, Z.L., Zhang, F.S., 2009. Reducing environmental risk by improving N management in intensive Chinese agricultural systems. Proc. Natl. Acad. Sci. USA 106, 3041–3046. https://doi.org/10.1073/pnas.0813417106.
Li, H., Wang, L., Peng, Y., Zhang, S., Lv, S., Li, J., Abdo, A.I., Zhou, C., Wang, L., 2021. Film mulching, residue retention, N fertilization affect ammonia volatilization through soil labile, N and C pools. Agric. Ecosyst. Environ. 308, 107272.
Liu, T.Q., Fan, D.J., Zhang, X.X., Chen, J., Li, C.F., Cao, C.G., 2015. Deep placement of nitrogen fertilizers reduces ammonia volatilization and increases nitrogen utilization efficiency in no-tillage paddy fields in central China. Field Crops Res. 184, 80–90.
Lundberg, S., 2018. SHAP documentation. https://shap.readthedocs.io/en/latest/. (Accessed 21 October 2025).
Lundberg, S.M., Lee, S.I., 2017. A unified approach to interpreting model predictions. In: Proceedings of the 31st International Conference on Neural Information Processing Systems (NIPS 2017), pp. 4765–4774. https://doi.org/10.5555/3295222.3295230. Long Beach, CA, USA.
Ma, R., Zou, J., Han, Z., Yu, K., Wu, S., Li, Z., Liu, S., Niu, S., Horwath, W.R., Zhu-Barker, X., 2021. Global soil-derived ammonia emissions from agricultural nitrogen fertilizer application: a refinement based on regional, crop-specific emission factors. Glob. Change Biol. 27, 855–867.
Massad, R.-S., Nemitz, E., Sutton, M.A., 2010. Review and parameterisation of bi-directional ammonia exchange between vegetation and the atmosphere. Atmos. Chem. Phys. 10, 10359–10386.
Misselbrook, T.H., Nicholson, F.A., Chambers, B.J., Johnson, R.A., 2005. Measuring ammonia emissions from land applied manure: an intercomparison of commonly used samplers and techniques. Environ. Pollut. 135, 389–397.

Molnar, C., 2020. Interpretable machine learning: a guide for making Black box models explainable self-published. Munich, Germany. https://christophm.github.io/interpretable-ml-book/.
MSZ, 1978. MSZ-08-0206/2-1978 Evaluation of Some Chemical Properties of the Soil Laboratory Tests (Ph Value, Phenolphthalein Alkalinity Expressed in Soda, Total Water Soluble Salt Content, Hydrolytic (Y1 Value) and Exchangeable Acidity (Y2 Value). Hungarian Standard Association, Budapest.
Nelson, A.J., Koloutsou-Vakakis, S., Rood, M.J., Myles, L., Lehmann, C., Bernacchi, C., Lin, J., 2017. Season-long ammonia flux measurements above fertilized corn in central Illinois USA using relaxed eddy accumulation. Agric. For. Meteorol. 239, 202–212.
Nemitz, E., Milford, C., Sutton, M.A., 2001. A two-layer canopy compensation point model for describing bi-directional biosphere–atmosphere exchange of ammonia. Q. J. R. Meteorol. Soc. 127, 815–833.
Pan, B., Lam, S.K., Mosier, A., Luo, Y., Chen, D., 2016. Ammonia volatilization from synthetic fertilizers and its mitigation strategies: a global synthesis. Agric. Ecosyst. Environ. 232, 283–289.
Personne, E., Loubet, B., Herrmann, B., Mattsson, M., Schjoerring, J.K., Nemitz, E., Sutton, M.A., Cellier, P., 2009. SURFATM NH_3: a model combining the surface energy balance and bidirectional exchanges of ammonia applied at the field scale. Biogeosciences 6, 1371–1388.
Philibert, A., Loyce, C., Makowski, D., 2013. Prediction of N_2O emission from local information with Random Forest. Environ. Pollut. 177, 156–163.
Qiao, C., Liu, L., Hu, S., Compton, J.E., Greaver, T.L., Li, Q., 2015. How inhibiting nitrification affects nitrogen cycle, reduces environmental impacts of anthropogenic nitrogen input. Glob. Change Biol. 21, 1249–1257.
Ren, C., Huang, X., Liu, T., Song, Y., Wen, Z., Liu, X., Ding, A., Zhu, T., 2023. A dynamic ammonia emission model and the online coupling with WRF-Chem (WRF-SoilN-Chem v1 0): development and evaluation. Geosci. Model Dev. Discuss. (GMDD) 2022, 1–29.
Rochester, I.J., Constable, G.A., MacLeod, D.A., 1991. Ammonia loss from soil during incubation and drying. Commun. Soil Sci. Plant Anal. 22, 1325–1334. https://doi.org/10.1080/00103629109368494.
Rochette, P., Angers, D.A., Chantigny, M.H., Gasser, M.O., MacDonald, J.D., Pelster, D.E., Bertrand, N., 2013. Ammonia volatilization, nitrogen retention: how deep to incorporate urea? J. Environ. Qual. 42, 1635–1642.
Rochette, P., MacDonald, J.D., Angers, D.A., Chantigny, M.H., Gasser, M.O., Bertrand, N., 2009. Banding of urea increased ammonia volatilization in a dry acidic soil. J. Environ. Qual. 38, 1383–1390.
Saha, D., Basso, B., Robertson, G.P., 2021. Machine learning improves predictions of agricultural nitrous oxide (N_2O) emissions from intensively managed cropping systems. Environ. Res. Lett. 16, 024004.
Sanz-Cobena, A., Lassaletta, L., Estellés, F., Del Prado, A., Guardia, G., Abalos, D., Aguilera, E., Pardo, G., Vallejo, A., Sutton, M.A., Garnier, J., Billen, G., 2014. Yield-scaled mitigation of ammonia emission from N fertilization: the Spanish case. Environ. Res. Lett. 9, 125005.
Scikit-learn Developers, 2025a. Cross decomposition in: Scikit-learn: machine learning in Python (Version 1.7.2). https://scikit-learn.org/1.7/modules/cross_decomposition.html. (Accessed 21 October 2025).
Scikit-learn Developers, 2025b. Cross-validation: evaluating estimator performance in: Scikit-learn: machine learning in Python (Version 1.7.2). https://scikit-learn.org/1.7/modules/cross_validation.html. (Accessed 21 October 2025).
Scikit-learn Developers, 2025c. Feature importance based on mean decrease in impurity (example "plot forest importances") in: Scikit-learn: machine learning in Python (Version 1.7.2). https://scikit-learn.org/stable/auto_examples/ensemble/plot_forest_importances.html. (Accessed 21 October 2025).
Scikit-learn Developers, 2025d. Linear models in: Scikit-learn: machine learning in Python (Version 1.7.2). https://scikit-learn.org/stable/modules/linear_model.html. (Accessed 21 October 2025).
Scikit-learn Developers, 2025e. Metrics and scoring: quantifying the quality of predictions (section 3.4.6) in: Scikit-learn: machine learning in Python (Version 1.7.2). https://scikit-learn.org/stable/modules/model_evaluation.html. (Accessed 21 October 2025).
Scikit-learn Developers, 2025f. Random forests and other randomized tree ensembles (section 1.11.2) in: Scikit-learn: machine learning in Python (Version 1.7.2). https://scikit-learn.org/stable/modules/ensemble.html#forest. (Accessed 21 October 2025).
Skiba, U., Jones, S.K., Dragosits, U., Drewer, J., Fowler, D., Rees, R.M., Pappa, V.A., Cardenas, L., Chadwick, D., Yamulki, S., Manning, A.J., 2012. UK emissions of the greenhouse gas nitrous oxide. Phil. Trans. Biol. Sci. 367, 1175–1185.
Sommer, S.G., Hutchings, N.J., 2001. Ammonia emission from field applied manure and its reduction. Eur. J. Agron. 15, 1–15.
Sommer, S.G., Schjoerring, J.K., Denmead, O.T., 2004. Ammonia emission from mineral fertilizers and fertilized crops. Adv. Agron. 82, 557–622.
Statista, 2025. https://www.statista.com/statistics/1266378/global-ammonia-production/.
Stryker, C., Lee, F., Bergmann, D., Scapicchio, M., 2025. The 2025 guide to machine learning IBM Think. https://www.ibm.com/think/topics/machine-learning. (Accessed 21 October 2025).
Sun, G.L., Zhang, Z.G., Xiong, S.W., Guo, X.Y., Han, Y.C., Wang, G.P., Feng, L., Lei, Y.P., Li, X.F., Yang, B.F., 2022. Mitigating greenhouse gas emissions, ammonia volatilization from cotton fields by integrating cover crops with reduced use of nitrogen fertilizer. Agric. Ecosyst. Environ. 332, 107946.
Sutton, M.A., Asman, W.A.H., Schjørring, J.K., 1994. Dry deposition of reduced nitrogen. Tellus B 46, 255–273.
Sutton, M.A., Reis, S., Riddick, S.N., Dragosits, U., Nemitz, E., Theobald, M.R., De Vries, W., 2013. Towards a climate-dependent paradigm of ammonia emission, deposition. Phil. Trans. Biol. Sci. 368, 20130166.
Uyekawa, J., Leland, J., Bergl, D., Liu, Y., Richardson, A.D., Lucas, B., 2025. Machine Learning-based prediction of ecosystem-scale CO_2 flux measurements. Land 14, 124.
Virtanen, P., Gommers, R., Oliphant, T.E., Haberland, M., Reddy, T., Cournapeau, D., Van Mulbregt, P., 2020. SciPy 1.0: fundamental algorithms for scientific computing in Python. Nat. Methods 17, 261–272.
Wan, X., Zhao, L., Wang, Z., Che, L., Xu, Y., Zhou, Y., Liu, Y., 2024. Effects of straw return, nitrogen application rates on soil ammonia volatilization, yield of winter wheat. Agronomy 14, 1469.
Wang, Y., Li, M., Yan, H., 2021. Ammonia volatilization from urea in alfalfa field with different nitrogen application rates, methods and timing. Agric. Ecosyst. Environ. 312, 107344. https://doi.org/10.1016/j.agee.2021.107344.
Xiang, J., Haden, V.R., Peng, S., Bouman, B.A., Huang, J., Cui, K., Visperas, R.M., Zhu, D., Zhang, Y., Chen, H., 2013. Effect of deep placement of nitrogen fertilizer on growth, yield, and nitrogen uptake of aerobic rice. Aust. J. Crop. Sci. 7, 870–877.
Zhan, X., Adalibieke, W., Cui, X., Winiwarter, W., Reis, S., Zhang, L., 2020. Improved estimates of ammonia emissions from global croplands. Environ. Sci. Technol. 55, 1329–1338.
Zhang, Z., Wang, J., Huang, W., Chen, J., Wu, F., Jia, Y., 2022. Cover crops, N fertilization affect soil ammonia volatilization, N_2O emission by regulating the soil labile carbon, nitrogen fractions. Agric. Ecosyst. Environ. 340, 108188. https://doi.org/10.1016/j.agee.2022.108188.
Zhong, X., Zhou, X., Fei, J., Huang, Y., Wang, G., Kang, X., Hu, W., Zhang, H., Rong, X., Peng, J., 2021. Reducing ammonia volatilization, increasing nitrogen use efficiency in machine-transplanted rice with side-deep fertilization in a double-cropping rice system in Southern China. Agric. Ecosyst. Environ. 306, 107183.
Zhou, P., Zhang, Z., Du, L., Sun, G., Su, L., Xiao, Z., Li, C., Wang, Z., Xiao, Z., Hu, T., Wang, K., Ni, F., Wang, S., Wang, H., 2022. Effect of deep placement of large granular fertilizer on ammonia volatilization, soil nitrogen distribution and rice growth. Agronomy 12, 2066.